Investigation of structural, morphological, optical and electrical properties of Co/Ni co-doped ZnO thin films

Noubeil Guermat [a],*, Warda Daranfed [b], Idris Bouchama [a], Nadir Bouarissa [c]

[a] Department of Electronics, Faculty of Technology, University of M'sila, M'sila 28000, Algeria
[b] Laboratory of Thin films and Interface, Faculty of Exact Science, Department of Physics, University of Constantine 1, Constantine 25000, Algeria
[c] Laboratory of Materials Physics and Its Applications, University of M'sila, M'sila 28000, Algeria

ARTICLE INFO

ABSTRACT

This work reports on the preparation and characterization of zinc oxide (ZnO) thin films using spray pyrolysis technique on glass substrates. The effect of cobalt and nickel doping and nickel/cobalt co-doping on the structural, optical, morphological and electrical properties of obtained films have been investigated. The obtained films are characterized by different techniques such as X-rays diffraction (XRD), UV-Visible, Scanning electron microscopy (SEM) and four probes electrical measurements. The results of the XRD characterization indicate that all the films of interest have the wurtzite hexagonal polycrystalline structure with (002) preferred orientation. Images of scanning electron microscopy (SEM) were used to observe the effect of doping and co-doping on films surface. Spectroscopy measurements in UV-VIS wavelength range have found to give good values of transmission (average value = 85%) for all elaborated layers, with a high transmission of 93% for the film deposited at 3%Ni. The films exhibit high transmittance around 85% with the presence of interference fringes in the visible region, indicating the films homogeneity and smoothness. The deduced optical gap values from optical measurement are found to be in the range of 3.26–3.30 eV. The electrical analysis shows that the conductivity increases with the co-doping compared to the pure ZnO film. The characterization of ZnO film co-doped 3%Ni:3%Co showed that the material under focus is a good candidate for optoelectronic applications such as the manufacture of solar cells with transparent electrodes.

1. Introduction

Zinc oxide with its chemical formula ZnO is a transparent material in the visible range. When doped, its large band gap allows it to be classified as transparent conductive oxides (TCO). Another major interest lies in the use of ZnO as a transparent conductor for making solar cells and flat panel display. To improve their electrical and optical properties from the point of view of specific applications, thin films of ZnO are often deliberately doped with group III elements (B, Al, In, Ga) and / or group IV elements (Pb, Sn). On the other hand, there is another TCO, quite common in the current optoelectronic industry: indium oxide doped with tin (In_2O_3:Sn or ITO) [1]. ITO is used, among other things, as electrodes for optoelectronic devices such as screens of cell phones or televisions. However, indium and gallium have significant drawbacks such as their high price and toxicity compared to other transition metals like Co and Ni. In this work, we have chosen cobalt as a dopant

because under light excitation, the Co^{+2} cation is ionized by forming the Co^{+3} cation. This ionization releases an electron which will be found in the conduction band [2]. This mechanism leads thus to an improvement in the electrical conductivity of films under light excitation [3]. In addition we have used nickel with ZnO [4] or SnO_2 [5] to improve transmittance. Moreover, the ionic radii of Ni^{+2} (0.055 nm) and Co^{+2} (0.058 nm) are comparable to Zn^{+2} (0.060 nm) [2,6]. In fact, much work on ZnO co-doped with Ni-Co has been reported in the literature for the ferromagnetic applications [7–9], nevertheless, in the current work we are interested in photovoltaic applications. Xu et al. [10] studied the influence of Ni (0, 1%, 3% and 5%) doping concentration on the structure and optical properties. Their results showed that the undoped and doped ZnO nanoparticles are both hexagonal wurtzite structures and the band gap energy decreases with increasing the concentration of Ni. Shukla et al. [11] have observed hexagonal wurtzite structure and more than 80% of transparency in the entire visible region of undoped and Co-doped (1%, 10%) ZnO thin films deposited by spin coating technique. Ali et al. [6] produced a ZnO co-doped Ni/Co film that had an optical gap from 3.55 to 3.71 eV by varying the

dopant concentrations. Mustafa et al. [7] investigated synthesis and characterization of optical band gap and electrical resistivity of thin films of $Zn_{0.9} Co_{0.1-x} Ni_x O$ (x = 0.0, 0.02, 0.04, 0.06, 0.08, 0.1) series which were deposited by Pulsed Laser deposition technique (PLD). Their findings showed that the band gap energy decreases from 3.09 to 3.03 eV and the resistivity increases as the Ni concentration is enhanced from x = 0.0 to 0.1. Many techniques can be used to deposit of Co-Ni doped ZnO thin films on glass substrates such as sol-gel processes [12–13], thermal evaporation process [14], pulsed laser deposition [15], chemical vapor deposition (CVD) [16] and spray pyrolysis [17]. Compared to other deposition techniques, spray pyrolysis technique was originally developed for the deposition of TCO material for solar cells. This technique has several advantages: it can be carried out at high surface; it facilitates the handling of precursors with the spray; it is a simple and economical (low-cost) technique.

The objective of this work is to study the structural, morphological, optical and electrical properties of Ni/Co co-doped ZnO thin films as a transparent electronic conductors and to compare their optoelectronic performance with those obtained in the literature.

2. Experimental procedure

ZnO films were prepared on glass substrates by pneumatic spray technique at different doping levels. The glass substrates are used to study the structural, electrical and optical properties with different doping elements. In the first step, the spray solution was prepared using 1.097 g of Zinc acetate dihydrate [$Zn(CH_3COO)_2.2H_2O$] as a precursor in 50 ml of methanol. After 10 min under magnetic stirring at room temperature, an adequate quantity of Cobalt ($CoCl_2H_2O$) and Nickel ($NiCl_26H_2O$) with a different doping rate (Co (1%), Ni (3%), Ni–Co (3%,2%), Ni–Co (3%,3%)) has been considered and a few drops of concentrated acetic acid solution has been added as a stabilizer. The solution mixture was stirred at 30°C for 2 h to yield a clear and transparent solution. The substrate temperature was fixed at 400°C, the carrier gas (compressed air) and the solution were fed into a spray nozzle at a pre-adjusted constant atomization pressure. The flow rate of solution was 8 ml/min. The nozzle to substrate distance was 17 cm and the diameter of the nozzle was 0.1 mm.

The structural properties were determined by XRD using a Philips X' Pert system with Cu Kα radiation ($\lambda CuK\alpha = 1.5418$Å). The optical transmission in the UV-Visible range (300–800 nm) measurements was performed using Shimadzu UV–3101 PC spectrophotometer. The surface morphology and microstructure were investigated by Scanning Electron Microscope embedded with EDX system. The electrical conductivity was calculated in the dark at room temperature and in a coplanar structure with two evaporated gold stripes attached to the films surface, where current-voltage (I (V)) characteristics were mainly made. By varying the bias voltage from 0 to 30 V, the current flowing in the sample is measured using a pico-ammeter (Keithley 617) which is able to measure currents up to 10^{-12} A.

3. Results and discussion

To compare the structural properties of different doping concentrations, we undertook X-ray measurements of pure ZnO thin films, ZnO:Co (1%), ZnO:Ni (3%), ZnO:NiCo (3%,2%) and ZnO:NiCo (3%,3%). The X-ray diffraction spectra of obtained films are shown in Fig. 1. It can be seen that all the films have five diffraction peaks located at 34.16°, 35.89°, 47.30°, 62.40° and 67.38° assigned to (002), (101), (102), (103) and (200) diffraction peaks, respectively. According to the ASTM files, JCPDS 36-1451 [18–19], the obtained films are polycrystalline with a Wurtzite hexagonal structure. The
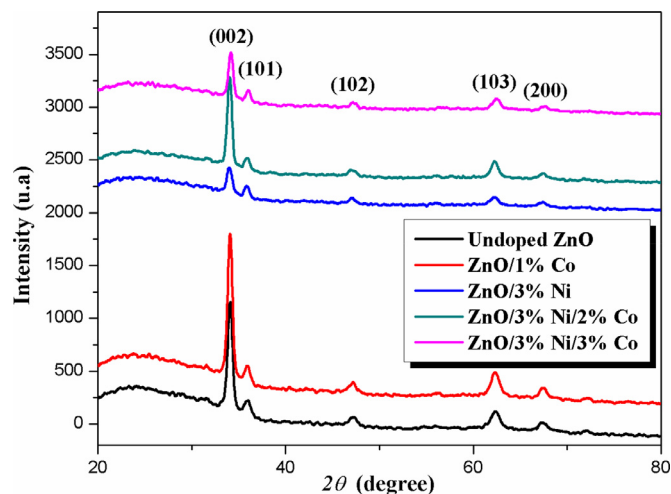

Fig. 1. X-ray diffraction spectra of obtained films with different doping and co-doping concentrations.
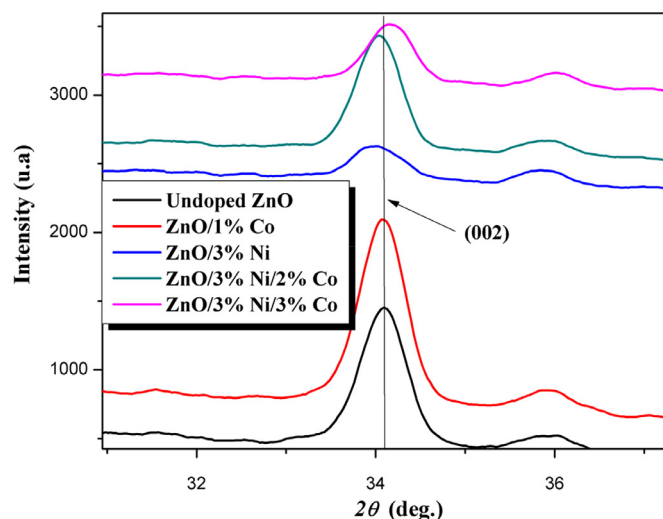

Fig. 2. Zoom of (002) Peak positions and intensities of X-ray diffraction of obtained films.

intense peak at (002) with an orientation located at 34.16° was observed for all samples. No secondary phases such as NiO, Co_3O_4, Co_2O_3 and CoO were detected. This indicates that the Zn ions have been substituted by the Co and Ni ions. This behavior accords well with that reported in the literature [20–21]. We noticed an increase of (002) peak intensity of ZnO:Co (1%) film with respect to that of pure ZnO film. This is probably due to the improvement of the films crystallinity. In addition, there is a decrease of (002) peak intensity of pure ZnO film with respect to those of ZnO:Ni (3%), Zno:NiCo (3%,2%) and Zno:NiCo (3%,2%) films. This reduction in the intensity of the peak (002) is due to the fact that it can be assigned to a smaller ionic radius of Ni^{+2} and Co^{+2} than that of Zn^{+2}, indicating that the Co^{+2} and Ni^{+2} ions are well incorporated in the ZnO matrix and occupy the Zn^{+2} sites. This behavior was already observed by Romeiro et al. [22] for Co, Ni co-doped ZnO layers prepared by microwave-assisted hydrothermal technique. According to Vijayaprasath et al. [23], this decrease indicates that the degree of crystallinity of the films decreases.

Fig. 2 presents a zoom of XRD spectra at (002) diffraction peak region for 2θ close to 31°-37°. As can be seen, a peak shift towards lower angles (34.10°, 34.08°, 33.98° and 34.04°) is appeared in samples of pure ZnO, ZnO:Co (1%), ZnO:Ni (3%) and ZnO:NiCo

Table 1
Crystallite sizes of doped and co-doped ZnO films.

Sample	FWHM	Crystallite size, (nm)	Dislocation density (δ), (nm)$^{-2}$	Strain (ε) $*10^{-3}$
Undoped ZnO	0.5056	16.440	0.00370	2.108
ZnO/1% Co	0.488	16.640	0.00203	3.611
ZnO/3% Ni	0.5339	15.565	0.00413	2.226
ZnO/3% Ni/2% Co	0.4854	17.123	0.00341	2.024
ZnO/3% Ni/3% Co	0.4837	17.188	0.00338	2.016

Table 2
Compositions of Co and Ni doped ZnO thin films at various concentrations.

Sample	%Zn	%O	%Co	%Ni
Undoped ZnO	22.51	59.43	-	-
ZnO/1% Co	28.44	61.43	0.95	-
ZnO/3% Ni	24.70	63.79	-	2.1
ZnO/3% Ni/2% Co	39.64	51.13	1.2	2.17
ZnO/3% Ni/3% Co	40.34	50.71	2.08	2.28

(3%,2%). Similar phenomenon has been observed by Bediaa et al. [24].

The crystallites sizes (D) corresponding to (002) orientation angel was estimated using the Scherrer formula [25]:

$$D = \frac{0.9\lambda}{\beta \cos\theta} \tag{1}$$

Where, λ is the wavelength of X-rays radiation, β represents the full width at half maximum (FWHM) and θ is the angle of diffraction.

The dislocation density (δ) is estimated by the following relation [26,27]:

$$\delta = \frac{1}{D^2} \tag{2}$$

The strain values (ε) of ZnO film along the plane (002) were calculated using the following formula:

$$\varepsilon = \frac{\beta \cos\theta}{4} \tag{3}$$

Table 1 summarizes the crystallites sizes (*D*), the dislocation density *(δ)* and the strain values *(ε)* at different doping and co-doping concentrations. We observe an increase in the crystallite size from 16.44 nm for pure ZnO film to 16.64 0nm for ZnO:Co (1%) film. This behavior may be due to the improvement of the structure crystallinity. For ZnO:Ni (3%) we observe a reduction in the crystallite size. The result found is in good agreement with the literature [28]. We can interpret the decrease in crystallites size by the nucleation center increase. In addition this decrease in the crystallites size with the increase in the strain leads to an increase in the number of defects in the crystal lattice such as dislocation density (Table 1). Similar behavior was also observed by M. Ashokkumar et al. for thin layers based on ZnO co-doped Cu and Ni deposited by the co-precipitation technique [29]. Generally, the defects on the grain surface suppress the nucleation and hence prevent the subsequent growth. According to Stolyarchuk et al. [30], this decrease is probably due to a certain quantity of Ni-dopant atoms preferring to locate in or near the grain boundary regions. In addition, an increase in the crystallite size of ZnO:NiCo (3%,2%) and ZnO:NiCo (3%,3%) were also observed. This increase in crystallite size is indicated by the decrease in structural defects which reduces in strain (Table 1) [31].

The morphology of undoped, doped 1%Co and co-doped 3%Ni:3%Co ZnO thin films was analyzed by Scanning Electron Microscopy (SEM) and shown in Fig. 3. As shown in figures undoped film is smooth, dense and continuous. The Co doping rends the

film composed of an uniform distribution of nanowire-like structure. However, the co-doping with Ni and Co the film surface roughness increase and the nanowire like structure becomes finer.

The EDX spectra of ZnO:NiCo (3%,3%) film is shown in Fig. 4. The composition studies by energy dispersive X-ray spectroscopy EDX (Table 2) show that the samples are quasi-stoichiometric and their compositions are rather similar to that of the source solution.

The transmission spectra (T) as a function of photons wavelength of films deposited on glass substrates at room temperature with wavelengths varied between 300-700 nm are shown in Fig. 5. We observed a high transparency for all samples with an average transmission of about 85% in the visible range. The value of the average transmission is about 87% and shows maximum value at co-doped 3%Co/3%Ni. High transparency is probably due to the low scattering effect resulting from the structural homogeneity of the layers and high bulk crystallinity (Table 1). The transmittance of ZnO doped Co films decreases compared to that of undoped ZnO film. This is due to the presence of more defects and interstitials in the ZnO: Co lattice. On the other hand, the value of the transmittance raises with ZnO/Ni (T = 93%, Fig. 5b) and the addition of a percentage of Co into ZnO/3%Ni leads to the increase of carrier concentrations in the lattices. Note that the transmission is slightly improved by Ni doping and co-doping Co/Ni, indicating a good incorporation of Cobalt and Nickel in the ZnO structure.

In order to estimate the value of the optical band gap energy for all samples of interest, we have used the Tauc relation [32]. This has been done by plotting $(\alpha h\nu)^2$ as a function of photon energy $h\nu$. The extrapolation of this curve gives the value of band gap energy as shown in Fig. 6.

$$(\alpha h\nu)^n = B(h\nu - E_g) \tag{4}$$

where E_g is the optical gap energy, α is the absorption coefficient, B is a constant and, $h\nu$ is the energy of the incident photon. We have also used the mathematical formula: $E = \frac{h.c}{\lambda}$ where h is Plank's constant, c is the speed of light, and λ is the absorption wavelength.

Table 3 regroups the values of E_g for different samples using Tauc relation and a mathematical formula. The variation of the optical band gap depends on various parameters such as the carrier concentration, the grains size, the deformation of lattice and the crystallites size. According to Table 3, the values of the optical gap energy varies in the range of 3.26–3.49 eV with the doping and co-doping concentrations. This variation is consistent with those reported in the literature [33–34]. The difference in the optical gap values obtained from the two methods mentioned above is due to the thickness. The increase in the optical gap is often reported in the literature and referred to as the Burstein-Moss effect for Co doped and co-doped (3%Ni/2%Co and 3%Ni/3%Co) compared to undoped ZnO films [35–36]. This may be due to the increase in the number of charge carriers (electrons) originating from the donor Co^{+2}, Ni^{+2} and Co^{+3} ions which are incorporated into the substitutional or interstitial locations of the Zn^{+2} cation. This variation of the optical gap of ZnO films as a function of Co/Ni co-doping is comparable to that reported in Ref. [6]. Nevertheless, on the contrary, Mustafa et al. [7] and Kocyigit et al. [37], have reported that the band gap energy of these materials decreases with the increase
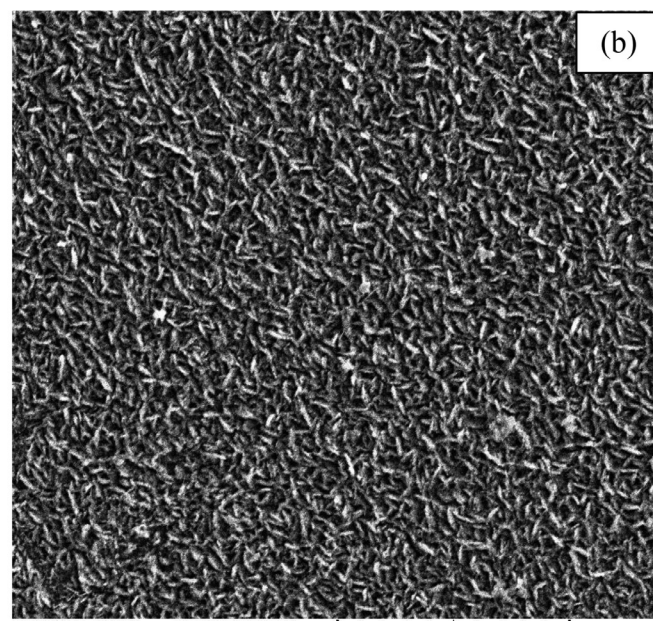
Table 3
Values of optical parameters of ZnO thin films deposited with different dopant and obtained from Tauc relation and a mathematical method.
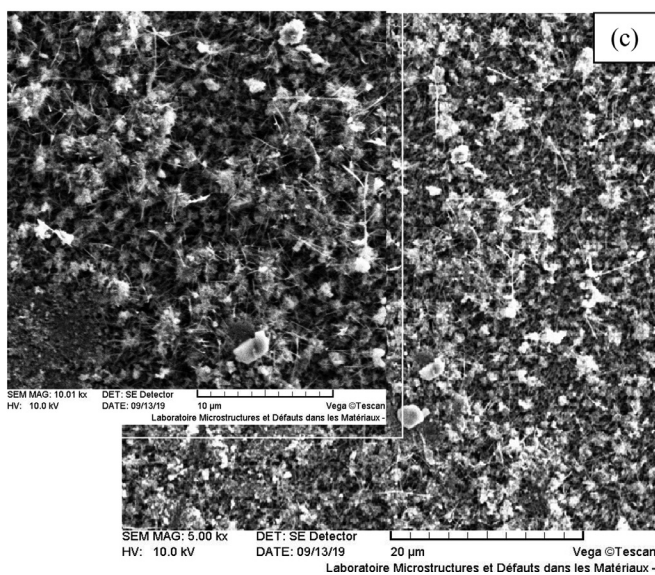
Sample	Wavelength, (nm)	Urbach energy, (meV)	Optical gap, (eV) calculated using Tauc relation	Optical gap, (eV) calculated using a mathematical method.
Undoped ZnO	367.81	324	3.27	3.37
ZnO/1% Co	364.60	321	3.28	3.40
ZnO/3% Ni	361.50	327	3.26	3.43
ZnO/3% Ni/2% Co	363.53	320	3.28	3.41
ZnO/3% Ni/3% Co	355.2	317	3.30	3.49
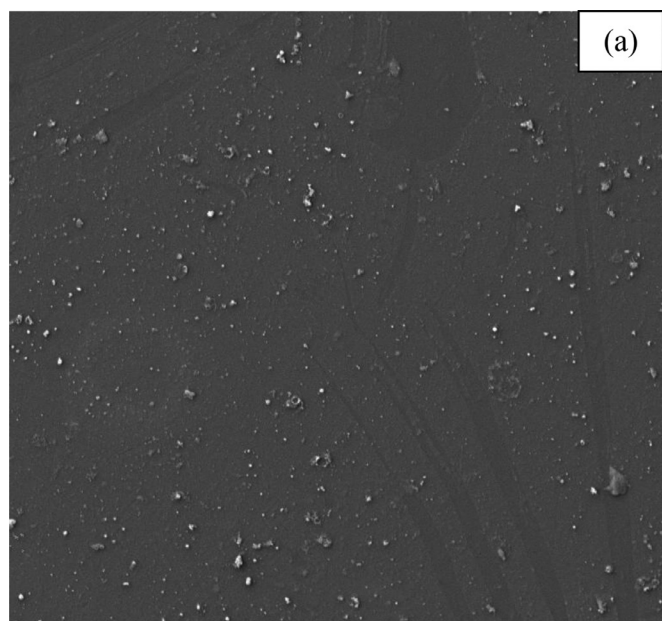
Fig. 3. Scanning electron micrographs of ZnO thin films with different concentrations, (a) Undoped, (b) 1%Co and (c) Ni:Co (3%,3%).
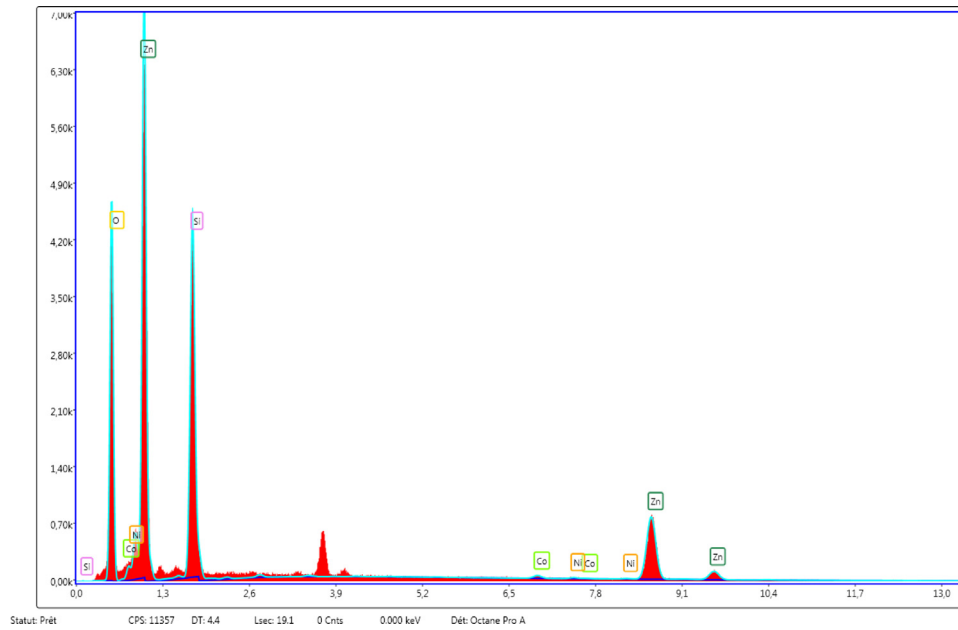
Fig. 4. EDX spectrum of ZnO thin films co-doping elements Ni:Co (3%,3%).
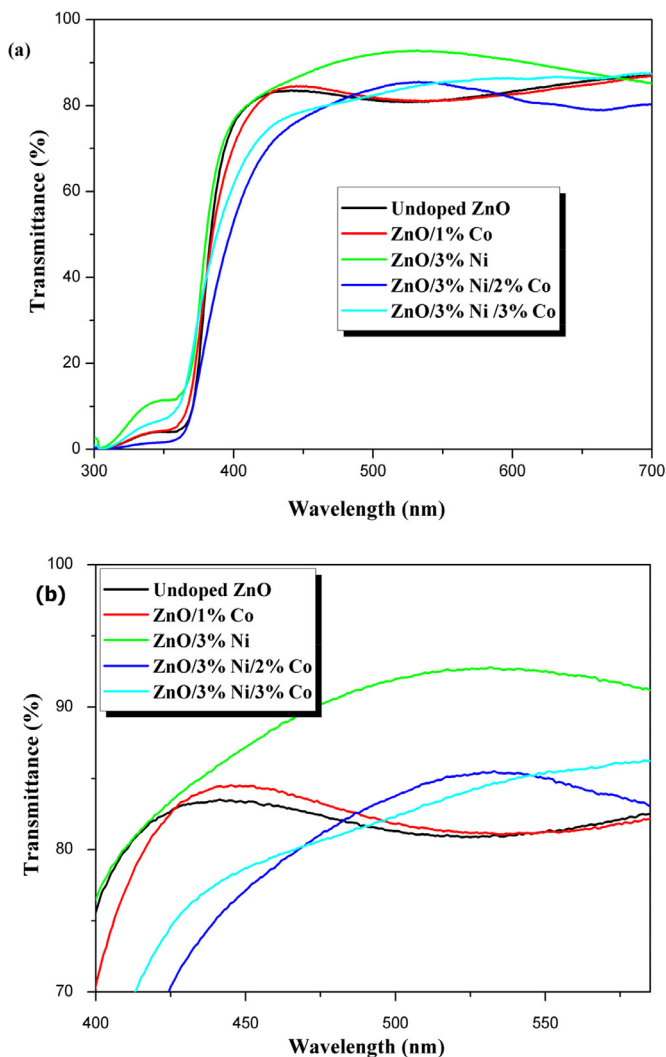

Fig. 5. (a) Transmission spectra of ZnO thin films deposited with different doping elements, (b) Magnified spectra from 400 to 490 nm.

in the concentration of Co/Ni. They attributed this decrease to be due to the sp-d exchange between d-band electrons located in the ZnO lattice and d electrons located in Ni^{+2} and Co^{+2} ions. Moreover, the variation of the optical gap is due to the increase in the crystallites size. We also noticed, for Ni-doped ZnO film, that there is a reduction in the optical gap compared to pure ZnO which is due to the appearance of electronic faults in the forbidden band. Guruvammal et al. [28] found a similar variation in the optical gap for ZnO: Ni films deposited by solvo-thermal method. According to Ali et al. [4], this decrease in band gap with the Ni doping is attributed to the exchange interaction between the d electrons associated with the doped Ni^{+2} cations and the s electrons or p holes near the strip edges. This behavior is due to the increase in strain (Table 1).

In order to estimate the disorder in the samples, we have used the Urbach energy. The estimation of the width of localized energy states was obtained by the Urbach energy. Generally, the width of localized states are laying into the forbidden energy gap [32].

$$\alpha = \alpha_0 \exp\left(\frac{h\nu}{E_u}\right) \tag{5}$$

Where E_U represents the Urbach energy, α is the absorption coefficient and α_0 is a constant. The Urbach energy values of the pure, doped and co-doped ZnO films are summarized in Table 3. We notice that the evolution of the Urbach energy is inversely proportional to that of the optical gap. The Urbach energy has a maximum value of 327 meV for Ni-doped ZnO (3%) film versus pure ZnO film. Minimum values of Urbach energy were obtained for other concentrations (Table 4). This behavior is probably due to the fact that doped Co and co-doped atoms have enough time to reorganize and occupy stable and favorable sites, which causes the occurrence of low density of structural defects characterized by a low energy Urbach in the film network.

The difference in the potential V between the two points is:

$$V = R.I \tag{6}$$

where,

I is the current which passes between the two points and R is the resistance of the layer.

The resistance of the intrinsic layer is calculated from the slope of the linear curve (I (V)). The calculation of the electrical conduc-

Table 4
Variation in electrical conductivity of undoped ZnO films, doped (Cobalt, Nickel) and co-doped (Ni-Co) with different percentages.

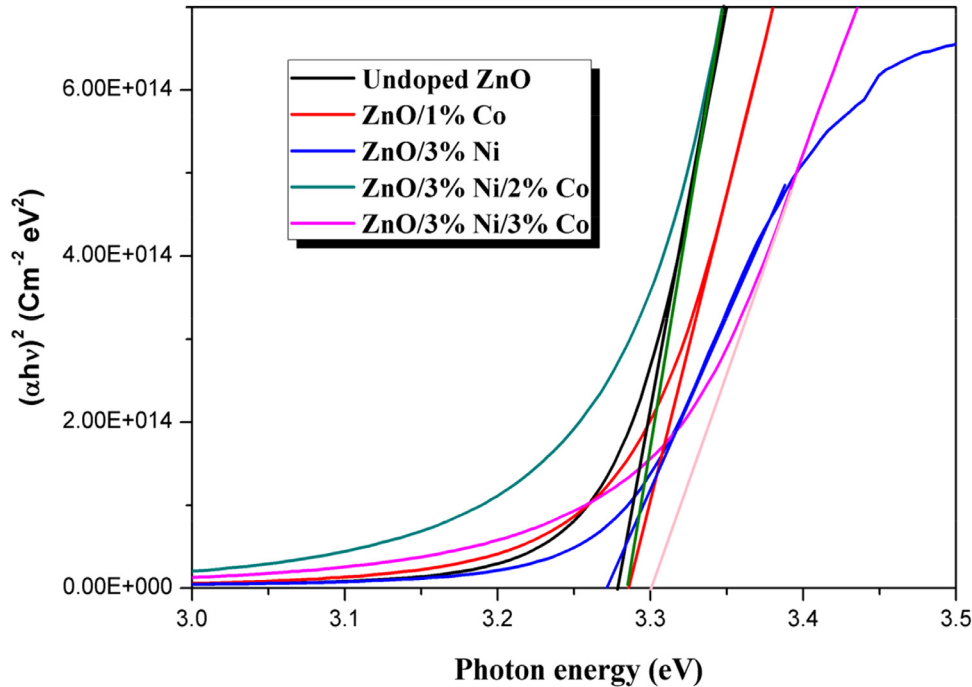| Sample	Resistance, 10^3 (Ω)	Thickness, (nm)	Conductivity, $(\Omega.cm)^{-1}$
Undoped ZnO	51.27	672.57	0.29
ZnO/1% Co	150.70	552.97	0.12
ZnO/3% Ni	3.60	765.22	3.63
ZnO/3% Ni/2% Co	0.37	617.90	43.74
ZnO/3% Ni/3% Co	0.29	513.44	67.16

Fig. 6. The $(\alpha h\upsilon)^2$ versus $h\upsilon$ curves of ZnO thin films deposited with different dopant for the optical energy gap calculation.

tivity depends on the electrical resistance R, on the intrinsic layer, as well as on the geometric parameters: inter-electrode distance L, the thickness d and the section of the conductive layer W. The conductivity σ, is related to these parameters by the following relation,

$$\sigma = \left(\frac{L}{W.D}\right)\left(\frac{1}{R}\right) \tag{7}$$

The electrical conductivity as a function of doping and co-doping percentages are summarized in Table 4. From Table 4, one can note the decrease in electrical conductivity for 1% Co doped film compared to an undoped ZnO film. This results is similar to the work of Godavarti et al. [38], ZnO films doped with small amounts cobalt have a higher resistivity. In our case, we noticed an increase of the conductivity for the 3%Ni doped film. The same behavior has been reported by Singh et al. [39]. The increase of the conductivity is attributed to the increase of electrons which are favored in the conduction band. The conductivity of all co-doped ZnO films is higher than those of pure ZnO and doped Co or Ni films. This is due to two reasons: the addition of Co into ZnO/3%Ni and the increase in the crystallite size (see Table 1). Mustafa et al. [7] reported a resistivity of 7.71×10^{-3} Ω.cm from a deposition by the PLD technique which seems to be larger than that of 1.48×10^{-2} Ω.cm obtained in this work. This difference in the resistivity is due to the technique used for the first time in this work which consists of adding Co in the Ni-doped ZnO film for the electrical study. Hence, one may conclude thus that the Ni:Co co-

doping improves the electrical conductivity of the materials under focus.

4. Conclusions

In this work, a comparative study on the structural, morphological, optical and electrical properties of thin films of undoped ZnO and doped with different dopants based on Co (1%), Ni (3%) and coblet-nickl co-doping was carried out. The aim of this contribution is to see the effect of co-doping on the physical properties for the possible use of the thin film of Ni/Co co-doped ZnO as transparent conductive oxides in solar cells. XRD analysis confirmed that the deposited films have a hexagonal Wurtzite structure with preferential orientation of (002) and no impurity phase was observed. The crystallite sizes are calculated using Debye-Scherrer formula, which shows that co-doped ZnO layers have the largest crystallite size. Scanning Electron Microscopy (SEM) showed that the film surface roughness increases and the nanowire like structure becomes finer for the layer co-doping with Ni and Co. The energy dispersive Xray spectra confirmed the presence of Ni and Co in the ZnO lattice. The UV-visible analysis showed that all the layers have a high transparency with an average transmission value of around 85%. However, the highest band gap value was obtained for the ZnO:NiCo (3%,3%) co-doped film. Electrical measurements were also carried out giving a minimum electrical resistivity of the order of 1.48×10^{-2} Ω.cm. In addition, we have observed that the thin layer of ZnO:Ni:Co (3%,3%) prepared by spray pyrolysis is transparent in the visible and has low resistivity, which suggests that our

production method makes it possible to obtain TCOs based on the ZnO layers for solar cells applications.

Declaration of Competing Interest

The authors declare that they have no known competing financial interests or personal relationships that could have appeared to influence the work reported in this paper.

Acknowledgments

References

[1] X. Xu, Z.Qi P.Wang, H. Ming, J. Xu, H. Liu, C. Shi, G. Lu andW. Ge, Formation mechanism of Zn$_2$SiO$_4$ crystal and amorphous SiO$_2$ in ZnO/Si system, J. Phys. Condens. Matter 15 (40) (2003) L607–L613.

[2] H.-J. Schulz, M. Thiede, Optical spectroscopy of 3d7 and 3d8 impurity configurations in a wide-gap semiconductor (ZnO:Co,Ni,Cu), Phys. Rev. B 35 (1987) 18–34.

[3] B. Demirselcuk, V. Bilgin, Ultrasonically sprayed ZnO:Co thin films: growth and characterization, Appl. Surf. Sci. 273 (2013) 478–483.

[4] H. Ali, A.M. Alsmadi, B. Salameh, M. Mathai, M. Shatnawi, N.M.A. Hadia, E.M.M. Ibrahim, Influence of nickel doping on the energy band gap, luminescence, and magnetic order of spray deposited nanostructured ZnO thin films, J. Alloys Compd. 816 (2020) 152538.

[5] M. Khalfallah, N. Guermat, W. Daranfed, N. Bouarissa, H. Bakhti, Hydrophilic nickel doped porous SnO$_2$ thin films prepared by spray pyrolysis, Phys. Scr. 95 (2020) 095805.

[6] R.N. Ali, H. Naz, J. Li, X. Zhu, P. Liu, B. Xiang, Band gap engineering of transition metal (Ni/Co) codoped in zinc oxide (ZnO) nanoparticles, J. Alloys Compd. 744 (2018) 90–95.

[7] L. Mustafa, S. Anjum, S. Waseem, S. Bashir, K. Mahmood, M. Saleem, E. Ahmad, Structural and optical properties of ZnO co-doped with Co and Ni thin films deposited by pulse laser deposition technique, Optik 161 (2018) 54–63.

[8] L. Mustafa, S. Anjum, S. Waseem, S. Javed, S.M. Ramay, S. Atiq, Effect of Co and Ni codoping on the structural, magnetic, electrical and optical properties of ZnO, Mater. Res. Bull. 84 (2016) 32–38.

[9] R.N. Aljawfi, S. Mollah, Properties of Co/Ni codoped ZnO based nanocrystalline DMS, J. Magn. Magn. Mater. 323 (2011) 3126–3132.

[10] K. Xu, C. Liu, R. Chen, X. Fang, X. Wu, J. Liu, Structural and room temperature ferromagnetic properties of Ni doped ZnO nanoparticles via low-temperature hydrothermal method, Physica B 502 (2016) 155–159.

[11] P. Shukla, S. Tiwari, S.R. Joshi, V.R. Akshay, M. Vasundhara, S. Varma, J. Singh, A. Chanda, Investigation on structural, morphological and optical properties of Co doped ZnO thin films, Physica B 550 (2018) 303–310.

[12] P.K.Shishodia Dhruvashi, Effect of cobalt doping on ZnO thin films deposited by sol-gel method, Thin Solid Films 612 (2016) 55–60.

[13] X.L. Zhang, K.S. Hui, F. Bin, K.N. Hui, L. Li, Y.R. Cho, R.S. Mane, W. Zhou, Effect of thermal annealing on the structural, electrical and optical properties of Al–Ni co-doped ZnO thin films prepared using a sol-gel method, Surf. Coat. Technol. 261 (2015) 149–155.

[14] S.H. Chiu, J.C.A. Huang, Chemical bath deposition of ZnO and Ni doped ZnO nanorod, J. Non-Cryst. Solids 358 (2012) 2453–2457.

[15] X. Wang, L. Zhu, L. Zhang, J. Jiang, Z. Yang, Z. Yea, B. He, Properties of Ni doped and Ni–Ga co-doped ZnO thin films prepared by pulsed laser deposition, J. Alloys Comp. 509 (2011) 3282–3285.

[16] Z.S. Min, Y.H. Lei, L.L. Sheng, C.X. Liang, L.S. Yun, H.Y. Ming, Y.R. Jian, L. Ning, Magnetic Properties of Ni-doped ZnO Nanocombs by CVD Approach, Nanoscale Res. Lett. 5 (2010) 1284–1288.

[17] S. Yılmaz, E. McGlynn, E. Bacaksız, J. Cullen, R.K. Chellappan, Structural, optical and magnetic properties of Ni-doped ZnO micro-rods grown by the spray pyrolysis method, Chem. Phys. Lett. 525–526 (2012) 72–76.

[18] H.S. Rasheed, N.M. Ahmed, M.Z. Matjafri, F.A. Sabah, N. Hamzah, The effect of the annealing on the properties of ZnO/Cu/ZnO multilayer structures, Procedia Chem. 19 (2016) 38–44.

[19] Q. Sun, G. Li, T. Tian, Z. Man, L. Zheng, M. Barré, J. Dittmer, F. Goutenoire, A.H. Kassiba, Controllable microstructure tailoring for regulating conductivity in Aldoped ZnO ceramics, J. Eur. Ceram. Soc. 40 (2020) 349–354.

[20] L. Bentes, R. Ayouchi, C. Santos, R. Schwarz, P. Sanguino, O. Conde, M. Peres, T. Monteiro, O. Teodoro, ZnO films grown by laser ablation with and without oxygen CVD, Super. Latt. Microstruct. 42 (2007) 152–157.

[21] F. Bittau, A. Abbas, K.L. Barth, J.W. Bowers, J.M. Walls, The effect of temperature on resistive ZnO layers and the performance of thin film CdTe solar cells, Thin Solid Films 633 (2017) 92–96.

[22] F.C. Romeiro, J.Z. Marinho, S.C.S. Lemos, A.P. de Moura, P.G. Freire, L.F. da Silva, E. Longo, R.A.A. Munoz, R.C. Lima, Rapid synthesis of Co, Ni co-doped ZnO nanoparticles: optical and electrochemical properties, J. Solid State Chem. 230 (2015) 343–349.

[23] G. Vijayaprasath, R. Murugan, S. Asaithambi, P. Sakthivel, T. Mahalingam, Y. Hayakawa, G. Ravi, Structural and magnetic behavior of Ni/Mn co-doped ZnO nanoparticles prepared by co-precipitation method, Ceram. Int. 42 (2016) 2836–2845.

[24] A. Bediaa, F.Z. Bedia, M. Aillerie, N. Maloufi, B. Benyoucef, Morphological and optical properties of ZnO thin films prepared by spray pyrolysis on glass substrates at various temperatures for integration in solar cell, Energy Procedia 74 (2015) 529–538.

[25] R. Zhang, M. Hummelgard, H. Olin, A facile one-step method for synthesising a parallelogram-shaped single-crystalline ZnO nanosheet, Mater. Sci. Eng. B 184 (2014) 1–6.

[26] M. Sathya, K. Pushpanathan, Synthesis and optical properties of Pb doped ZnO nanoparticles, Appl. Surf. Sci. 449 (2018) 346–357.

[27] W. Daranfed, N. Guermat, K. Mirouh, Experimental study in the effect of precursors in Co$_3$O$_4$ thin films used as solar absorbers, Annales de Chimie - Science des Matériaux 44 (2020) 121–126.

[28] D. Guruvammal, S. Selvaraj, S. Meenakshi Sundar, Effect of Ni-doping on the structural, optical and magnetic properties of ZnO nanoparticles by solvothermal method, J. Alloys Comp. 682 (2016) 850–855.

[29] M. Ashokkumar, S. Muthukumaran, Microstructure, optical and FTIR studies of Ni, Cu co-doped ZnO nanoparticles by co-precipitation method, Opt. Mater. 37 (2014) 671–678.

[30] I.D. Stolyarchuk, G.I. Kleto, A. Dziedzic, Structural and optical properties of Co and Ni doped ZnO thin films prepared by RF magnetron sputtering, Phys. Chem. Solid State 18 (2017) 302–308.

[31] A. GuruSampath Kumar, X. Li, Y. Du, Y. Geng, X. Hong, UV-photodetector based on heterostructured ZnO/(Ga,Ag)-co-doped ZnO nanorods by cost-effective two-step process, Appl. Surf. Sci. 509 (2020) 144770.

[32] W. Daranfed, M.S. Aida, A. Hafdallah, H. Lekiket, Substrate temperature influence on ZnS thin films prepared by ultrasonic spray, Thin Solid Films 518 (2009) 1082–1084.

[33] S. Jagtap, K.R. Priolkar, Evaluation of ZnO nanoparticles and study of ZnO-TiO$_2$ composites for lead free humidity sensors, Sens. Actuators B 183 (2013) 411–418.

[34] Y. Aoun, B. Benhaoua, S. Benramache, B. Gasmi, Effect of annealing temperature on structural, optical and electrical properties of zinc oxide (ZnO) thin films deposited by spray pyrolysis technique, Optik 126 (2015) 5407–5411.

[35] M. Arshad, A. Azam, A.S. Ahmed, S. Mollah, A.H. Naqvi, Effect of Co substitution on the structural and optical properties of ZnO nanoparticles synthesized by sol–gel route, J. Alloys Comp. 509 (2011) 8378–8381.

[36] R. Baghdad, N. Lemée, G. Lamura, A. Zeinert, N. Hadj-Zoubir, M. Bousmaha, M.A. Bezzerrouk, H. Bouyanfif, B. Allouche, K. Zellama, Structural and magnetic properties of Co-doped ZnO thin films grown by ultrasonic spray pyrolysis method, Superlattices Microstruct. 104 (2017) 553–569.

[37] A. Kocyigit, R. Topkaya, Structural, optical and magnetic properties of Ni-Co co-doped ZnO thin films, Mater. Res. Express 6 (2019) 096116.

[38] U. Godavarti, V.D. Mote, M. Dasari, Role of cobalt doping on the electrical conductivity of ZnO nanoparticles, J. Asian Ceram. Soc. 5 (2017) 391–396.

[39] S. Singh, N. Rama, M.S. Ramachandra Rao, Influence of d-d transition bands on electrical resistivity in Ni doped polycrystalline ZnO, Appl. Phys. Lett. 88 (2006) 222111.